Dia1 and IQGAP1 interact in cell migration and phagocytic cup formation

Dominique T. Brandt,[1] Sabrina Marion,[2] Gareth Griffiths,[2] Takashi Watanabe,[3] Kozo Kaibuchi,[3] and Robert Grosse[1]

[1]Institute of Pharmacology, University of Heidelberg, 69120 Heidelberg, Germany
[2]European Molecular Biology Laboratory Heidelberg, 69117 Heidelberg, Germany
[3]Department of Cell Pharmacology, Nagoya University Graduate School of Medicine, Nagoya, Aichi 466-8550, Japan

The Diaphanous-related formin Dia1 nucleates actin polymerization, thereby regulating cell shape and motility. Mechanisms that control the cellular location of Dia1 to spatially define actin polymerization are largely unknown. In this study, we identify the cytoskeletal scaffold protein IQGAP1 as a Dia1-binding protein that is necessary for its subcellular location. IQGAP1 interacts with Dia1 through a region within the Diaphanous inhibitory domain after the RhoA-mediated release of Dia1 autoinhibition. Both proteins colocalize at the front of migrating cells but also at the actin-rich phagocytic cup in macrophages. We show that IQGAP1 interaction with Dia1 is required for phagocytosis and phagocytic cup formation. Thus, we identify IQGAP1 as a novel component involved in the regulation of phagocytosis by mediating the localization of the actin filament nucleator Dia1.

Introduction

Regulation of the actin cytoskeleton is a key mechanism for the control of cell shape and motility involved in numerous complex and dynamic processes such as cell polarization, adhesion, endocytosis, and phagocytosis. These events require the localization and activation of specific actin nucleation factors to generate de novo actin filament networks of different sizes and shapes. The intensively studied actin-related protein 2/3 (Arp2/3) complex generates branched actin filaments, whereas the family of formin proteins produces unbranched actin filaments (for reviews see Pollard and Borisy, 2003; Harris and Higgs, 2004). The Diaphanous-related formins (DRFs) stimulate barbed end actin filament elongation through the dimeric formin homology (FH) 2 domain preceded by a proline-rich FH1 domain (Xu et al., 2004; Otomo et al., 2005; Kovar et al., 2006). Dia1 is characterized by regulatory domains in which the N terminus encompasses a RhoA-binding domain (RBD) followed by a four armadillo repeat–containing Diaphanous inhibitory domain (DID) that binds the C-terminal Diaphanous autoregulatory domain (DAD), thereby maintaining the protein in a dormant conformation (Lammers et al., 2005; Kovar, 2006). Dia1 autoinhibition between DAD and DID was shown to be released through the binding of RhoA-GTP to the RBD (Lammers et al., 2005). The armadillo repeat–containing DID and the adjacent dimerization domain have also been called the FH3 region and are thought to be involved in subcellular DRF location through interaction with unknown factors (Zigmond, 2004). Thus, targeting of Dia1 to actin dynamic regions is not yet understood but likely involves activated RhoA (Goulimari et al., 2005). The proposed biological functions of mammalian Dia1 so far are rather diverse and include cell adhesion and migration, microtubule stabilization, serum response factor (SRF) transcriptional activity, and endocytosis and phagocytosis (Faix and Grosse, 2006).

Phagocytosis is the activity performed by professional phagocytes to engulf large particles (>0.5 μm). This activity is crucial for tissue homeostasis and clearance of pathogenic microorganisms. Dia1 has been shown to be essential for CR3-mediated phagocytosis in macrophages, which is a Rho-mediated process (Colucci-Guyon et al., 2005). The DRF FRLα (formin-related gene in leukocytes α) is required for Fcγ receptor–mediated phagocytosis in macrophages, which is a Cdc42/Rac-mediated process (Caron and Hall, 1998; Seth et al., 2006). Both DRFs are recruited at the phagocytic cup, where de novo actin polymerization occurs during pseudopod extension around the particle. It has been suggested that N-WASP (neural Wiskott Aldrich syndrome protein) and the Arp2/3 complex activate actin nucleation at the nascent phagosome in both CR3 and RFcγ-mediated phagocytosis. The precise role of DRFs during phagocytic cup formation is still unknown but likely involves the regulation of actin dynamics or the de novo assembly of actin filaments together with the Arp2/3 complex.

Correspondence to Robert Grosse: Robert.Grosse@pharma.uni-heidelberg.de

Abbreviations used in this paper: Arp2/3, actin-related protein 2/3; DAD, Diaphanous autoregulatory domain; DBR, Dia1-binding region; DID, Diaphanous inhibitory domain; DRF, Diaphanous-related formin; F-actin, filamentous actin; FH, formin homology; RBD, RhoA-binding domain; SRF, serum response factor.

The online version of this article contains supplemental material.

The Journal of Cell Biology, Vol. 178, No. 2, July 16, 2007 193–200
http://www.jcb.org/cgi/doi/10.1083/jcb.200612071

In this study, we identify IQGAP1 as a new binding partner of Dia1. IQGAP1 regulates Dia1 localization at the leading edge of migrating cells as well as at the phagocytic cup in macrophages. Furthermore, we show that the deregulation of IQGAP1 activity fully inhibited phagocytosis in mouse macrophages, thus suggesting a crucial role for this protein in the immune response.

Results and discussion

Identification of IQGAP1 as a Dia1-binding protein

To identify factors responsible for the localization and regulation of DRFs, we used GST affinity columns containing an N-terminal region of Dia1 spanning amino acids 256–567 (formerly FH3). Using that approach, we eluted a specific band migrating at 190 kD from HeLa cell extracts (Fig. 1 A). Mass spectrometric analysis identified this band as the cytoskeletal scaffold protein IQGAP1 (Fig. S1, available at http://www.jcb.org/cgi/content/full/jcb.200612071/DC1), and these data were confirmed by immunoblotting using an IQGAP1-specific antiserum (Fig. 1 B). IQGAP1 is a widely expressed Rac and Cdc42-binding protein that is involved in polarized cell migration by regulating microtubule capture through CLIP170 and adenomatosis polyposis coli (Fukata et al., 2003; Watanabe et al., 2004). Furthermore, IQGAP1 is enriched at cell–cell contact sites as well as at the leading edge of migrating cells, where it influences the actin cytoskeletal morphology through mechanisms that are less well understood (Brown and Sacks, 2006). However, it has recently been shown that IQGAP1 binds N-WASP and, thereby, activates Arp2/3-mediated actin nucleation (Le Clainche et al., 2006).

The fact that IQGAP1 and Dia1 both influence the actin filament and the microtubule system in migrating cells led us to further characterize a possible relationship between these two cytoskeletal regulators. First, we tested whether endogenous Dia1 and IQGAP1 would associate using immunoprecipitations from serum-starved and -stimulated cells. Interestingly, detectable coprecipitated IQGAP1 increased by 3.4 ± 0.9-fold within 10 min in a serum-dependent manner (Fig. 1 C), suggesting that extracellular signals dynamically regulate the association of Dia1 with IQGAP1. Second, immunofluorescence analysis on wounded migrating fibroblasts confirmed that endogenous IQGAP1 accumulates at the leading edge, where it colocalizes with microinjected Dia1-FH3, whereas this construct did not inhibit cell migration (Fig. 1 D). These data suggest that this N-terminal region mediates the interaction of Dia1 with IQGAP1 in polarized cell movement. Interestingly, recent data demonstrated that active RhoA and Dia1 colocalize at the leading front of migrating cells, and this Dia1 localization

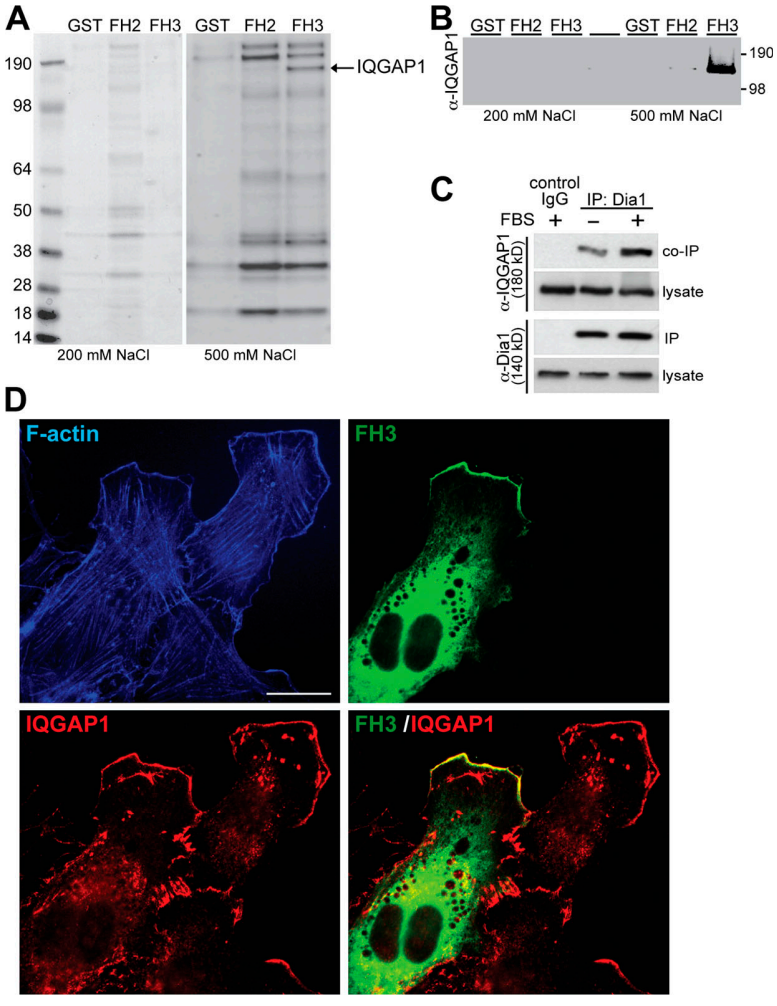

Figure 1. **Identification of IQGAP1 as a Dia1-binding protein.** (A) HeLa cell lysate was applied to glutathione–Sepharose bead resin columns loaded with GST, GST-FH2, or GST-FH3. Bound proteins were eluted by 200 and 500 mM NaCl and analyzed by SDS-PAGE and Coomassie staining. (B) An aliquot of the eluate was analyzed by immunoblotting using antibodies specific for IQGAP1. (C) HeLa cells were treated with 10% FBS or left untreated before immunoprecipitation for Dia1 or control IgG. 5% of total cell extracts and 30% of immunoprecipitation (IP) reactions were analyzed by immunoblotting as indicated. (D) Myc-Dia1-FH3 plasmids were microinjected into NIH3T3 cells located in the front row of a wounded monolayer 30 min after wounding. 3 h later, cells were stained for myc, F-actin, and IQGAP1. Bar, 10 μm.

depends on activated RhoA (Goulimari et al., 2005), indicating that RhoA regulates Dia1 activity in this specific location. Indeed, when cells were treated with C3 to inactivate RhoA, Dia1 no longer localized to the wound edge of migrating cells as expected, whereas IQGAP1 localization to the leading edge was unaffected (unpublished data). Thus, Dia1 and IQGAP1 associate dynamically during cell migration, and localization of Dia1 but not IQGAP1 depends on RhoA activation at the front of protruding cells.

The C terminus of IQGAP1 binds the armadillo repeat region of Dia1

In an attempt to characterize the domains responsible for association with Dia1, we generated a series of IQGAP1 mutants according to known domain boundaries (Fig. 2 A) and performed coimmunoprecipitation experiments in HEK293 cells. The FH3 region was reciprocally immunoprecipitated with IQGAP1 and interacted preferentially with the C terminus of IQGAP1 (Fig. 2, B and C). These data also revealed that IQGAP1 interacted specifically with Dia1 or its N-terminal region but not with Dia2 or Dia3 (Fig. 2, C and D), whereas both IQGAP1 and IQGAP2 coimmunoprecipitated with the FH3 region (Fig. S2 A, available at http://www.jcb.org/cgi/content/full/jcb.200612071/DC1). The minimal IQGAP1-binding region of Dia1 spans amino acids 256–346, representing the armadillo repeats 3 and 4 of the N-terminal region (Lammers et al., 2005), and it is both sufficient and required for IQGAP1 binding (Fig. 2 E). The Dia1-binding region (DBR) of IQGAP1 lies within the IQGAP1 C terminus (Fig. S2, B and C) and was narrowed down to a recombinantly purifiable fragment of amino acids 1,503–1,657. In vitro binding studies with purified N-terminus Dia1 (Dia1-nt) and IQGAP1 DBR revealed a single class of affinity binding sites with a K_D of ~60 nM (Fig. 2 F). This IQGAP1 C-terminal region was previously reported to bind to the armadillo repeat domain of adenomatosis polyposis coli (Watanabe et al., 2004), suggesting a similar mode of protein–protein interaction as observed for Dia1. Interestingly, the DBR directly interacted with Dia1-nt that was dependent on the release of C-terminus Dia1 (Dia1-ct)–mediated

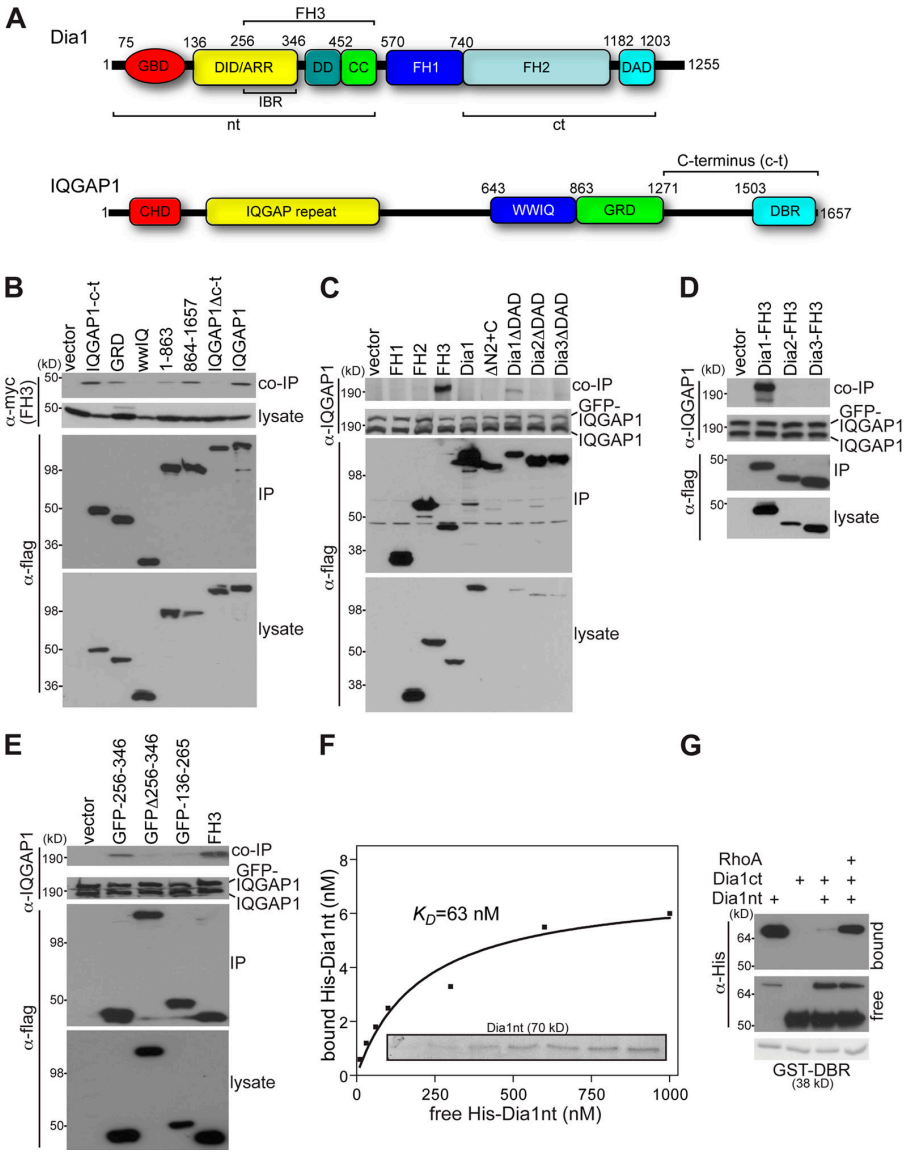

Figure 2. **IQGAP1 binds the armadillo repeat of Dia1.** (A) Schematic representation of Dia1 and IQGAP1. (B) Flag-IQGAP1 constructs were transfected in HEK293 cells with myc-FH3. (C) Indicated Dia1 mutants were transfected with GFP-IQGAP1. (D) Dia1 mutants were transfected with GFP-IQGAP1. (E) Flag-Dia1 constructs were transfected with GFP-IQGAP1. (B–E) Cell extracts were incubated using α-Flag-agarose and analyzed by immunoblotting as indicated. (F) Increasing concentrations of recombinant His–Dia1-nt were incubated with 60 μM of immobilized GST-DBR, the amounts of bound Dia1-nt were visualized by Coomassie staining, and the K_D value was calculated by nonlinear regression analysis. The results are representative of three independent experiments. (G) Association of GST-DBR to Dia1-nt depends on Dia1-ct–mediated autoinhibition and its release by RhoAV14. Purified proteins were analyzed by immunoblotting (α-His). Coomassie staining for GST-DBR is shown (bottom). One representative experiment out of three independent experiments is shown.

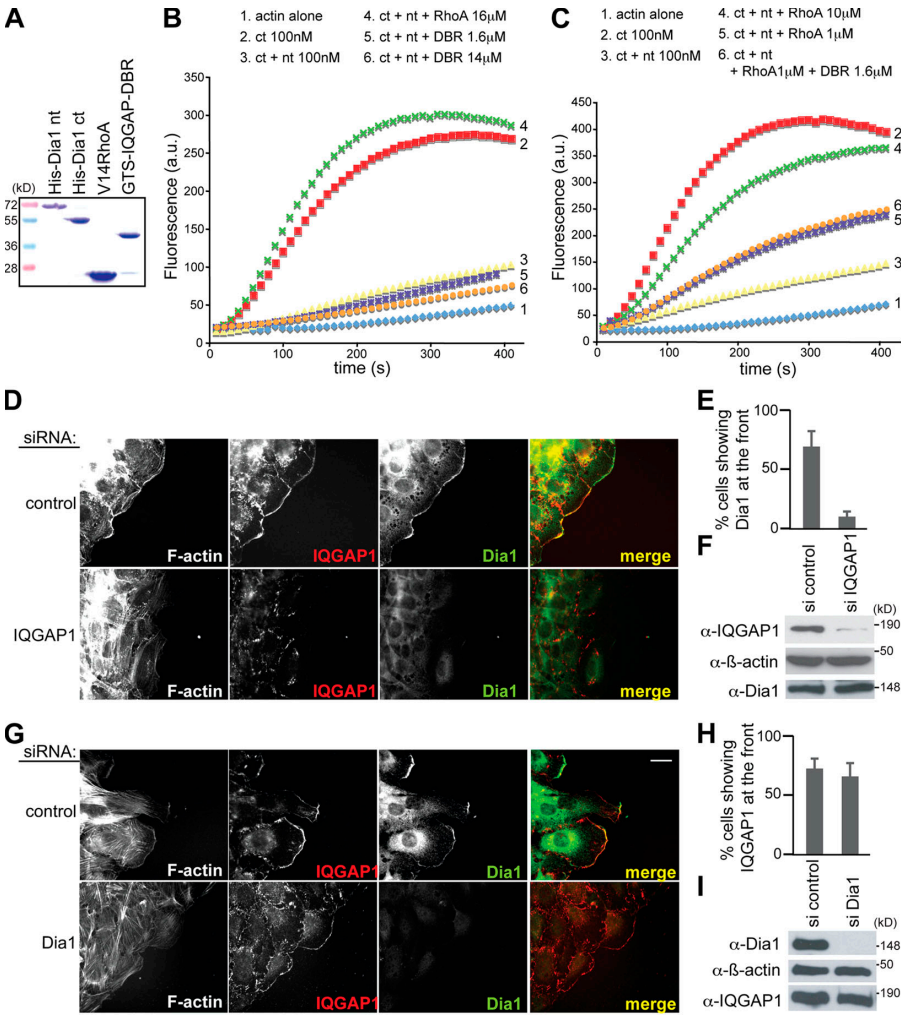

Figure 3. **IQGAP1 is required for localization but does not activate or inhibit Dia1.** (A) Coomassie-stained SDS-PAGE of 1–2 μg of proteins used in B. (B and C) Pyrene actin assembly assays containing 4 μM actin (5% pyrene labeled) and purified components as indicated. (D) NIH3T3 cells were transfected with either control or siRNAs specific for IQGAP1 (siRNA #2) for 48 h before wounding. Cells were fixed 4 h after wounding and analyzed for IQGAP1 and Dia1 using specific antibodies. (E) Dia1 localization at the wound edge was determined by scoring a minimum of 100 cells. (F) Cells were treated as in D, lysed, and the indicated proteins were analyzed by immunoblotting. (G) NIH3T3 cells were transfected with either control or siRNA specific for Dia1 for 48 h before wounding. Cells were fixed 4 h later and analyzed for IQGAP1 and Dia1 using specific antibodies. (H) IQGAP1 localizations to the wound edge were quantified as in E. (I) Cells were treated as in G, lysed, and the amount of Dia1 as well as the indicated controls were analyzed by immunoblotting as indicated. (E and H) Values represent means ± SD (error bars) of three independent experiments. Bar, 10 μm.

autoinhibition by the addition of active RhoA, whereas it did not interact with autoinhibited Dia1-nt/Dia1-ct in the absence of RhoA (Fig. 2 G), demonstrating that only activated Dia1 associates with IQGAP.

IQGAP1 does not activate or inhibit Dia1

Because the Dia1–IQGAP1-binding region partially overlaps with regulatory domains such as the DAD–DID autoinhibitory binding interface, we tested whether the DBR of IQGAP1 directly affects the actin polymerizing activity of Dia1 in vitro. For this, we functionally reconstituted Dia1 autoinhibition using N- and C-terminal constructs. The N-terminal construct contains the RBD, DID, dimerization domain, and the coiled-coil regions, and the C-terminal construct spans the FH2 and DAD domains (Fig. 2 A). As reported by Li and Higgs (2005), we observed that the C terminus stimulates actin filament assembly, which can be inhibited by the N terminus (Fig. 3, A and B). The addition of purified V14RhoA fully restored FH2-mediated actin polymerization in a dose-dependent manner, whereas the addition of IQGAP1-DBR displayed no detectable effects on Dia1-mediated actin filament assembly either alone or in combination with RhoA (Fig. 3, B and C). Consistent with this, IQGAP1 or its C terminus neither stimulated SRF nor interfered with Dia1-induced SRF activity (Fig. S2 D), which is known to depend on actin dynamics (Posern and Treisman, 2006). Thus, although only RhoA-activated Dia1 binds IQGAP1, we observed that IQGAP1 neither activated nor inhibited actin polymerization by Dia1. Of course, this does not rule out that full-length IQGAP1 can modulate Dia1 activity under more physiological conditions (for example, to stabilize its active conformation).

IQGAP1 is required for the localization of Dia1

Because the FH3 of Dia1 colocalized with IQGAP1 at the front of migrating cells, we speculated that IQGAP1 is involved in the subcellular location of Dia1. To test this, NIH3T3 cells were treated with control siRNA or with siRNA specific for Dia1 or IQGAP1, and monolayers were scratch wounded to induce polarized cell migration. Previous RNAi studies demonstrated a critical role for both proteins in wounding-induced fibroblast cell migration (Watanabe et al., 2004; Goulimari et al., 2005). Using this assay, we observed that localization of Dia1 to the wound edge of migrating cells depends on the presence of IQGAP1, but, when Dia1 was knocked down, IQGAP1 localization was normal (Fig. 3, D–I). In agreement with this, we found that cells expressing the DBR failed to localize Dia1 to the wound edge (Fig. S2 E).

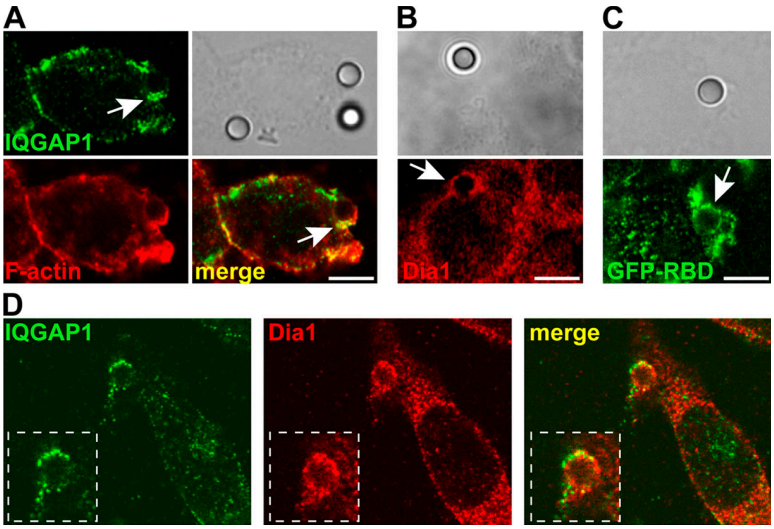

Figure 4. **IQGAP1, Rho-GTP, and Dia1 are components of the phagocytic cup.** RAW macrophages were incubated with 3-μm avidin-coated beads for 15 min before fixation and immunostaining. Beads were visualized by phase contrast. All images represent a single confocal plan. (A) IQGAP1 (green) and F-actin (red) colocalize at the phagocytic cup during bead internalization (arrows). (B and C) Dia1 (B) and active Rho, which was detected by using recombinant GFP-RBD (C), are enriched at the phagocytic cup. Arrows indicate localization at the phagocytic cup. (D) The colocalization of Dia1 (red) and IQGAP1 (green) at the phagocytic cup is shown (merge). Boxed areas are magnifications of the phagocytic cup. Bars, 5 μm.

This argues that IQGAP1 is required to localize Dia1 at the front of the migrating cell.

IQGAP1, Rho-GTP, and Dia1 are components of the phagocytic cup

The front of migrating cells is a cortical region of high local actin filament assembly and disassembly (for review see Pollard and Borisy, 2003). Using RNAi, it has recently been suggested that Dia1 is involved in phagocytosis by a yet unidentified mechanism (Colucci-Guyon et al., 2005). Therefore, we decided to investigate the potential role of IQGAP1 in localizing Dia1-mediated actin filament assembly by studying phagocytic cup formation, a process in which localized actin polymerization provides the driving force by which cells internalize particles (Chimini and Chavrier, 2000). First, we examined IQGAP1 and Dia1 localization during the internalization of 3-μm avidin-coated latex beads in RAW macrophages. Avidin coating stimulates internalization via unknown receptors. Immunofluorescence analysis showed that endogenous IQGAP1 localizes to the phagocytic cup of avidin-coated beads along with filamentous actin (F-actin; Fig. 4 A) as well as to CR3-coated beads (not depicted). Likewise, we also observed a distinct signal for endogenous Dia1 around the phagocytic cup (Fig. 4 B), indicating that Dia1 functions locally at these structures. Consistent with this, using a previously described in situ probe for Rho-GTP (Goulimari et al., 2005), we could detect active Rho at the phagocytic cup, suggesting that it may promote local Dia1 activation during phagocytosis. Further supporting these findings are the observations that IQGAP1 and Dia1 colocalize at the phagocytic cup (Fig. 4 D). These data suggest that Dia1 and IQGAP1 interact during phagocytic cup formation, as observed at the leading edge of migrating cells, and that RhoA is also locally activated to promote internalization. Thus, IQGAP1 localization at the phagocytic cup may be essential for positioning RhoA-induced Dia1 activity.

Association of IQGAP1 with Dia1 is indispensable for phagocytosis

We examined the localization of IQGAP1 during phagocytosis in a more dynamic way by expressing GFP-IQGAP1 in macrophages. We confirmed that GFP-IQGAP1 but not GFP is recruited to the phagocytic cup (Fig. 5, A and B). After phagocytic closure, IQGAP1 was not detected around the internalized phagosome (Fig. 5 B, asterisk). However, on a later stage of maturation, we observed that some phagosomes exhibited rocketing movement throughout the cell cytoplasm, which was characterized by the formation of an actin tail (Fig. 5 C and Video 1, available at http://www.jcb.org/cgi/content/full/jcb.200612071/DC1). This phenomenon has been observed for endosomes and more recently for phagosomes in *Dictyostelium discoideum* (Clarke et al., 2006). We could monitor such phenomenon in RAW macrophages stably expressing GFP-actin (Video 1). To our surprise, we observed that GFP-IQGAP1 is enriched in the comet tails during phagosome rocketing (Fig. 5 C and Video 2). This implies that IQGAP1 is involved in different phagocytosis stages in which actin filament assembly is required, suggesting a critical function of IQGAP1 for activating local de novo actin nucleation. Rocketing movement of phagosomes likely does not involve microtubules, suggesting that IQGAP1 could act in the cell as a regulator of actin assembly independently of its function as a microtubule plus end–capturing protein.

To investigate the functional role of the IQGAP1–Dia1 interaction in phagocytosis, we overexpressed the IQGAP1-DBR in RAW macrophages. In contrast to wild-type IQGAP1, which localized to the plasma membrane and to filopodia, this domain showed a diffuse distribution throughout the cytoplasm (Fig. 5 D). We observed that cells expressing the IQGAP1-DBR were unable to initiate phagocytic cup formation and to subsequently take up opsonized particles (Fig. 5 E). However, binding of the beads to the surface of the cell was not impaired (Fig. 5 D, arrows). Furthermore, in DBR-expressing cells, endogenous IQGAP1 still localized to the cell cortex (Fig. 5 D, top). In contrast, Dia1 showed a diffuse distribution throughout the cytoplasm and was not detected at the bead-binding site (Fig. 5 D, bottom). These data suggest that the DBR can function as an interfering version of IQGAP1, probably by inhibiting its interaction with endogenous Dia1, and show that this interaction is crucial to initiate phagocytic cup formation.

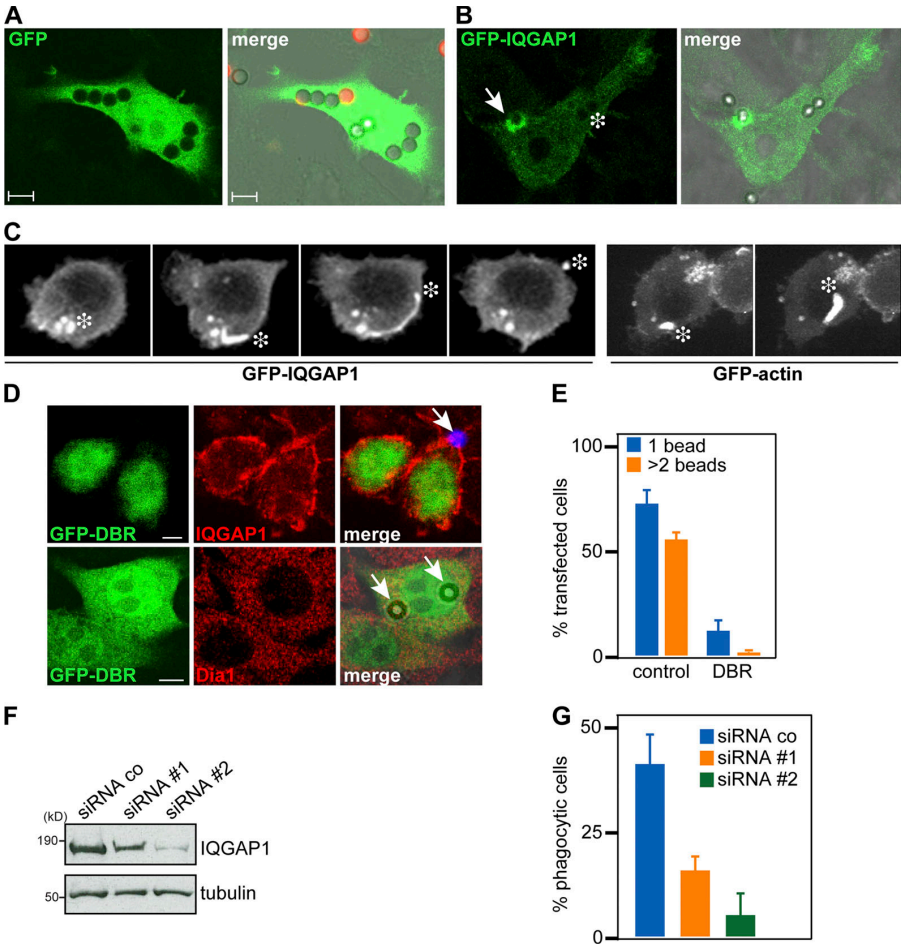

Figure 5. **Association of IQGAP1 with Dia1 is indispensable for phagocytosis.** (A and B) RAW macrophages were transfected with GFP (A) as a control or GFP-IQGAP1 (B; green) before incubation with 3-μm avidin-coated beads for 15 min. GFP expression does not interfere with bead binding at the membrane (red) or phagocytosis (internalized beads observed by phase contrast). IQGAP1 is recruited at the phagocytic cup (arrow) but is not detected around internalized beads (asterisk). (C) GFP-IQGAP1– and GFP-actin–expressing macrophages showed the recruitment of actin and IQGAP1 in the tail of 1-μm rocketing phagosomes. Asterisks indicate the positions of the rocketing phagosome in each video still. (D) RAW macrophages were transfected with GFP-DBR (green), incubated with 3-μm avidin-coated beads for 1 h, fixed, and immunostained for Dia1 or IQGAP1 (red). Membrane-attached beads (noninternalized) are indicated by arrows (top, α-avidin in blue). (E) The percentage of positive transfected cells either with GFP or GFP-DBR displaying one or more than two internalized beads per cell. (F) IQGAP1 protein expression in RAW cells transfected with control siRNA or two different siRNA specific for IQGAP1 (#1 and #2). (G) The graph shows the percentage of siRNA-treated cells with at least one internalized avidin-coated bead after 1 h of incubation. All quantifications shown are the means ± SD (error bars) of three independent experiments. Bars, 5 μm.

To confirm the functional role of IQGAP1 in phagocytosis, we inhibited IQGAP1 production using two different siRNAs. Western blot analysis showed that IQGAP1 expression was decreased by 50% in cells treated with siRNA #1 and for 90% in cells treated with siRNA #2 (Fig. 5 F). The IQGAP1 knocked down cells showed an almost complete inhibition of phagocytic activity (Fig. 5 G), demonstrating the crucial role of IQGAP in the phagocytic process.

In this study, we identify IQGAP1 as a binding partner for Dia1 and as a novel regulator for phagocytosis. The interaction of IQGAP1 and Dia1 appears to be critical for phagocytic cup formation, implicating IQGAP proteins as factors that regulate Dia1 localization in addition to or in cooperation with RhoA, thereby adding another level of complexity in how cells control formin function. Thus, it is tempting to speculate that local actin polymerization by Dia1 acts as a driving force for phagocytosis. Interestingly, a recent report has demonstrated that the Cdc42-regulated DRF FRLα is important for phagocytosis and has suggested that, in addition to GTPase activity, a factor X may bind at the DRF N terminus to promote membrane localization (Seth et al., 2006). In the case of Dia1, we would like to propose that IQGAP1 represents such a factor. Because IQGAP specifically binds Dia1 but not Dia2 or Dia3, it is likely that different scaffold proteins regulate other DRFs in a specific manner for various cellular functions involving cytoskeletal dynamics.

Materials and methods

Reagents and antibodies

All cell culture reagents were obtained from Invitrogen. All chemicals were obtained from Sigma-Aldrich. 3 μm of latex beads were purchased from Polyscience. HRP-conjugated α-Flag, α-myc antibodies, and α-Flag agarose were purchased from Sigma-Aldrich, monoclonal α-Dia1 antibodies were obtained from BD Biosciences, and α-His antibodies were purchased from QIAGEN. α-Dia1 antibodies were raised in rabbits against synthetic peptides representing residues 727–765 and were purified using affinity chromatography on immobilized peptides. Generation of IQGAP1 antiserum was described previously (Fukata et al., 2002). All secondary antibodies were obtained from Dianova. IQGAP2 cDNA was a gift from A. Bernards (Massachusetts General Hospital, Boston, MA), and pGEX-RhoAV14 was a gift from J. Faix (Medizinische Hochschule Hannover, Hannover, Germany).

Plasmids

Desired IQGAP and Dia plasmids were amplified by PCR using specific primers (Table S1, available at http://www.jcb.org/cgi/content/full/jcb.200612071/DC1). To obtain Dia1 plasmids deleted for residues 256–346 or 750–770, the corresponding codons were replaced with three alanines, introducing a Not1 site.

Bacterial expression and protein purification

Proteins were purified in the *Escherichia coli* strain DE3 using standard protocols (Brandt et al., 2003). Proteins were dialyzed against 25 mM Tris, pH 7.4, 50 mM NaCl, 2 mM EDTA, 2 mM DTT, and 2% glycerol. His-tagged Dia1-ct (748–1,203) and -nt (1–548) were prepared according to Li and Higgs (2005).

Dia1 binding studies

9×10^9 Hela cell extracts (Cil) were lysed with a Dounce homogenizer, and lysates were cleared by centrifugation at 100,000 *g* and passed through glutathione beads to remove endogenous GST. 25 mg/ml of cell

extracts was incubated with 0.5 mg GST fusion proteins coupled to glutathione–Sepharose beads and eluted by salt gradient before isopropanol precipitation. Eluates were analyzed by SDS-PAGE (4–12% Bis-Tris gels; Invitrogen) and colloidal Coomassie. Protein bands of interest were excised and analyzed by mass spectrometry (matrix-assisted laser desorption/ionization-time of flight; Biochemiezentrum Heidelberg).

Cells, transfections, stainings, and image analysis

RAW 264.1 mouse macrophages, NIH3T3, and HEK293 cells were maintained in DME supplemented with 10% FBS, 2 mM glutamine, 100 IU/ml penicillin, and 100 mg/ml streptomycin at 37°C in a CO^2 atmosphere. Cells were transfected using LipofectAMINE 2000 (Invitrogen). IQGAP1-specific siRNA (#2, 5′-UUAUCGCCCAGAAACAUCUUGUUGG-3′; and #1, 5′-UUCUUCAUGAGACAAGGCUUGUUCA-3′) was obtained from Invitrogen, and Dia1 siRNA (Arakawa et al., 2003; Goulimari et al., 2005; Eng et al., 2006) was obtained from IBA. Wound-healing assays and stainings on NIH3T3 cells were performed as described previously (Goulimari et al., 2005). RAW cells grown on 12-mm glass coverslips were incubated with 3 μm of latex beads coated with avidin (1:100 final dilution) in internalization medium (MEM, 10 mM Hepes, and 5 mM D-glucose, pH 7.4). Cells were fixed and permeabilized before PFA was quenched in 50 mM PBS/NH_4Cl for 15 min. Staining of F-actin was performed by incubating the cells with 0.5 μM phalloidin-TRITC for 30 min at RT. Detection of IQGAP1 and Dia1 was performed by incubating cells for 1 h at RT with polyclonal α-IQGAP1 antibodies (dilution of 1:100) or monoclonal α-p140mDia antibodies (1:100). For RhoA-GTP detection, purified GFP-RBD protein was added at a final concentration of 0.02 mg/ml for 2 h at 4°C as described previously (Goulimari et al., 2005). Slides were mounted in MOWIOL. Immunofluorescence images were collected with a microscope (DMIRE2; Leica) equipped a camera (DC350F; Leica) and IM50 imaging software (Leica) or with an FCS confocal laser-scanning microscope (LSM510; Carl Zeiss MicroImaging, Inc.) equipped with an oil immersion UV PLAPO 63× NA 1.32 lens (Carl Zeiss MicroImaging, Inc.). Images were processed using Photoshop CS (Adobe).

Coimmunoprecipitations and protein interactions

Cell extracts were subjected to immunoprecipitation and immunoblotting as described previously (Grosse et al., 2003). For in vitro interactions, increasing concentrations of purified His–Dia1-nt were mixed with immobilized GST-DBR in binding buffer (20 mM Tris-HCl, pH 8, 100 mM NaCl, 0.1% CHAPS, 0.1% Triton X-100, and 1 mM DTT), and bound proteins were analyzed by Coomassie brilliant blue staining. The amount of His–Dia1-nt was detected in a linear range using serial dilutions of standards (BSA) by Coomassie staining and was estimated by densitometric analysis using Photoshop (Adobe). Nonlinear regressions were determined using Prism software (GraphPad). To reconstitute Dia1 autoinhibition, 0.03 μM His–Dia1-nt was incubated in the absence or presence of 0.06 μM His–Dia1-ct or His–Dia1-ct together with 3 μM V14RhoA for 10 min on ice. GST-DBR–coupled glutathione–Sepharose beads were added, and reactions were incubated for 30 min at 4°C. Precipitates were washed four times, and proteins were analyzed by immunoblotting.

Actin assembly assays

Protein solutions were mixed with 40 μl of G buffer (20 μM $CaCl_2$, 20 μM ATP, and 0.5 mM Tris-HCl, pH 8) and 10 μl of polymerization buffer (12.5 mM KCl, 0.5 mM $MgCl_2$, 2and 5 μM ATP) and added to 30 μl of G actin (5% pyrene labeled; final concentration of 4 μM; Cytoskeleton, Inc.). Pyrene fluorescence was excited at 365 nm and recorded at 407 nm every 12.5 s for a period of 500 s for every experiment.

Live cell imaging

48 h after transfection, RAW cells were replated onto 35-mm glass-bottom dishes and allowed to adhere for 8 h. For imaging, cells were placed at 37°C on a heated stage connected to a humidifier module. To start phagocytosis, cells were incubated with 1 ml of imaging medium (10 mM Hepes and 5 mM D-glucose, pH 7.4) containing latex beads coupled to avidin. Imaging runs were started after bead internalization. For each time point, a 10-plan z stack of GFP images spaced 0.5 μm apart was acquired at an exposure time of 500 ms for GFP-actin–expressing cells and at 800 ms for GFP-IQGAP1 cells. A total of 10 images per time point were collected, which resulted in one time point per 5 s for actin-GFP and 8 s for IQGAP-GFP. Beads were visualized in the GFP channel as a result of their autofluorescence.

Phagocytosis assay

48 h after transfection, RAW cells grown on 12-mm glass coverslips were incubated at 37°C with 3-μm latex beads coated with avidin (1:100 final dilution) in internalization medium (MEM, 10 mM Hepes, and 5 mM D-glucose, pH 7.4). After 1 h, cells were washed and fixed with 4% PFA. Noninternalized beads were stained using either biotin-rhodamine or monoclonal α-avidin antibody (1:100) detected by α-mouse-Cy5. Internalized beads were counted using phase contrast. Three independent experiments were performed. For each, 30 cells positive for GFP-protein transfection were examined for their phagocytic activity.

Online supplemental material

Fig. S1 represents the peptide sequences of IQGAP1 identified by mass spectrometric analysis. Fig. S2 shows Dia1-IQGAP interaction and its effects on SRF activity and Dia1 localization in migrating cells. Table S1 provides detailed information about the plasmids generated in this study. Video 1 shows phagosome rocketing in a GFP-actin–expressing RAW cell. Video 2 reveals the presence of GFP-IQGAP1 during phagosome rocketing. Online supplemental material is available at http://www.jcb.org/cgi/content/full/jcb.200612071/DC1.

We thank T. Kurzchalia for critical reading of the manuscript. We thank S. Narumiya, A. Bernards for plasmids, and J. Faix for pGexRhoV14 and advice on actin assembly assays. We thank A. Gille, D. Holzer, and A. Rippberger for technical assistance and thank laboratory members for discussions. We further thank an anonymous reviewer for pointing us to the experiments in Fig. 2 G.

S. Marion is a recipient of a Marie Curie postdoctoral fellowship. This work was supported by the Emmy Noether Program of the Deutsche Forschungsgemeinschaft (grant GR2111/1-2 to R. Grosse).

Submitted: 14 December 2006
Accepted: 14 June 2007

References

Arakawa, Y., H. Bito, T. Furuyashiki, T. Tsuji, S. Takemoto-Kimura, K. Kimura, K. Nozaki, N. Hashimoto, and S. Narumiya. 2003. Control of axon elongation via an SDF-1α/Rho/mDia pathway in cultured cerebellar granule neurons. *J. Cell Biol.* 161:381–391.

Brandt, D.T., A. Goerke, M. Heuer, M. Gimona, M. Leitges, E. Kremmer, R. Lammers, H. Haller, and H. Mischak. 2003. Protein kinase C delta induces Src kinase activity via activation of the protein tyrosine phosphatase PTP alpha. *J. Biol. Chem.* 278:34073–34078.

Brown, M.D., and D.B. Sacks. 2006. IQGAP1 in cellular signaling: bridging the GAP. *Trends Cell Biol.* 16:242–249.

Caron, E., and A. Hall. 1998. Identification of two distinct mechanisms of phagocytosis controlled by different Rho GTPases. *Science*. 282:1717–1721.

Chimini, G., and P. Chavrier. 2000. Function of Rho family proteins in actin dynamics during phagocytosis and engulfment. *Nat. Cell Biol.* 2:E191–E196.

Clarke, M., A. Muller-Taubenberger, K.I. Anderson, U. Engel, and G. Gerisch. 2006. Mechanically induced actin-mediated rocketing of phagosomes. *Mol. Biol. Cell*. 17:4866–4875.

Colucci-Guyon, E., F. Niedergang, B.J. Wallar, J. Peng, A.S. Alberts, and P. Chavrier. 2005. A role for mammalian diaphanous-related formins in complement receptor (CR3)-mediated phagocytosis in macrophages. *Curr. Biol.* 15:2007–2012.

Eng, C.H., T.M. Huckaba, and G.G. Gundersen. 2006. The formin mDia regulates GSK3beta through novel PKCs to promote microtubule stabilization but not MTOC reorientation in migrating fibroblasts. *Mol. Biol. Cell*. 17:5004–5016.

Faix, J., and R. Grosse. 2006. Staying in shape with formins. *Dev. Cell*. 10:693–706.

Fukata, M., T. Watanabe, J. Noritake, M. Nakagawa, M. Yamaga, S. Kuroda, Y. Matsuura, A. Iwamatsu, F. Perez, and K. Kaibuchi. 2002. Rac1 and Cdc42 capture microtubules through IQGAP1 and CLIP-170. *Cell*. 109:873–885.

Fukata, M., M. Nakagawa, and K. Kaibuchi. 2003. Roles of Rho-family GTPases in cell polarisation and directional migration. *Curr. Opin. Cell Biol.* 15:590–597.

Goulimari, P., T.M. Kitzing, H. Knieling, D.T. Brandt, S. Offermanns, and R. Grosse. 2005. Galpha12/13 is essential for directed cell migration and localized Rho-Dia1 function. *J. Biol. Chem.* 280:42242–42251.

Grosse, R., J.W. Copeland, T.P. Newsome, M. Way, and R. Treisman. 2003. A role for VASP in RhoA-Diaphanous signalling to actin dynamics and SRF activity. *EMBO J.* 22:3050–3061.

Harris, E.S., and H.N. Higgs. 2004. Actin cytoskeleton: formins lead the way. *Curr. Biol.* 14:R520–R522.

Kovar, D.R. 2006. Molecular details of formin-mediated actin assembly. *Curr. Opin. Cell Biol.* 18:11–17.

Kovar, D.R., E.S. Harris, R. Mahaffy, H.N. Higgs, and T.D. Pollard. 2006. Control of the assembly of ATP- and ADP-actin by formins and profilin. *Cell*. 124:423–435.

Lammers, M., R. Rose, A. Scrima, and A. Wittinghofer. 2005. The regulation of mDia1 by autoinhibition and its release by Rho*GTP. *EMBO J.* 24:4176–4187.

Le Clainche, C., D. Schlaepfer, A. Ferrari, M. Klingauf, K. Grohmanova, A. Veligodskiy, D. Didry, D. Le, C. Egile, M.F. Carlier, and R. Kroschewski. 2006. IQGAP1 stimulates actin assembly through the N-WASP-ARP2/3 pathway. *J. Biol. Chem.* 282:426–435.

Li, F., and H.N. Higgs. 2005. Dissecting requirements for auto-inhibition of actin nucleation by the formin, mDia1. *J. Biol. Chem.* 280:6986–6992.

Otomo, T., D.R. Tomchick, C. Otomo, S.C. Panchal, M. Machius, and M.K. Rosen. 2005. Structural basis of actin filament nucleation and processive capping by a formin homology 2 domain. *Nature*. 433:488–494.

Pollard, T.D., and G.G. Borisy. 2003. Cellular motility driven by assembly and disassembly of actin filaments. *Cell*. 112:453–465.

Posern, G., and R. Treisman. 2006. Actin' together: serum response factor, its cofactors and the link to signal transduction. *Trends Cell Biol.* 16:588–596.

Seth, A., C. Otomo, and M.K. Rosen. 2006. Autoinhibition regulates cellular localization and actin assembly activity of the diaphanous-related formins FRLalpha and mDia1. *J. Cell Biol.* 174:701–713.

Watanabe, T., S. Wang, J. Noritake, K. Sato, M. Fukata, M. Takefuji, M. Nakagawa, N. Izumi, T. Akiyama, and K. Kaibuchi. 2004. Interaction with IQGAP1 links APC to Rac1, Cdc42, and actin filaments during cell polarization and migration. *Dev. Cell*. 7:871–883.

Xu, Y., J.B. Moseley, I. Sagot, F. Poy, D. Pellman, B.L. Goode, and M.J. Eck. 2004. Crystal structures of a Formin Homology-2 domain reveal a tethered dimer architecture. *Cell*. 116:711–723.

Zigmond, S.H. 2004. Formin-induced nucleation of actin filaments. *Curr. Opin. Cell Biol.* 16:99–105.